Focusing inside an unknown medium using reflection data with internal multiples: numerical examples for a laterally-varying velocity model, spatially-extended virtual source, and inaccurate direct arrivals

Filippo Broggini and Roel Snieder, Center for Wave Phenomena - Colorado School of Mines;*
Kees Wapenaar, Delft Univ. of Technology

SUMMARY

Seismic interferometry is a technique that allows one to reconstruct the full response from a virtual source inside a medium, assuming a receiver is present at the virtual source location. We describe a method that creates a virtual source inside a medium from reflection data measured at the surface, without needing a receiver inside the medium and, hence, presenting an advantage over seismic interferometry. An estimate of the direct arriving wavefront is required in addition to the reflection data. However, no information about the medium is needed. We illustrate the method with numerical examples in a lossless acoustic medium with laterally-varying velocity and density and take into consideration finite acquisition aperture and a spatially-extended virtual source. We examine the reconstructed wavefield when a macro model is used to estimate the direct arrivals. The proposed method can serve as a basis for data-driven suppression of internal multiples in seismic imaging.

INTRODUCTION

We present and discuss a new approach to retrieve the full response from a virtual source $\mathbf{x}_{VS}$ inside a medium and, consequently, to focus the wavefield at the virtual source location. Conventional methods for seismic interferometry (Curtis et al., 2006; Bakulin and Calvert, 2006; Schuster, 2009) allow one to reconstruct such a response without knowing the medium parameters, but these methods necessitate a receiver in the subsurface at the location of the virtual source and assume that sources surround the medium. The approach that we propose removes the constraint of having a receiver at the virtual source location and is based on a development of the 1D theory previously proposed by Broggini et al. (2011, 2012) and Broggini and Snieder (2012)[1]. Given the reflection response of a 1D medium, they show that it is possible to reconstruct the response originating from a virtual source inside the medium, without the presence of a receiver at the virtual source location and without knowing the medium.

A first attempt to generalize the 1D method to three-dimensional media was made by Wapenaar et al. (2011a). Using physical arguments, they proposed an iterative scheme that transforms the reflection response of a 3D medium (measured at the $z = 0$) into the response to a virtual source located inside the unknown medium. Additionally, the proposed method requires an estimate of the direct arrivals propagating between the virtual source location and the acquisition surface (besides the reflection data measured at the surface). These direct arrivals represents a key element of the method because they specify the location and the spatial extent of the virtual source in the subsurface. Due to this reason, the proposed method is not fully model-independent. A model that relates the direct arrivals to a virtual source position is, however, simpler than a model that correctly handles the internal multiples.

[1] Broggini et al., 2012, submitted to Geophysics.

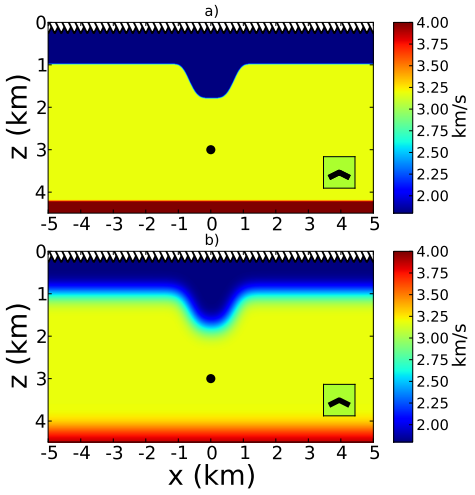

Figure 1: (a) True velocity model with a syncline reflector. (b) Smooth velocity model used to model the first arrivals between the virtual source location $\mathbf{x}_{VS}$ and the acquisition surface at $z = 0$. In both panels, the black dot represents the location of the extended virtual source used in the first numerical example. The square inset (bottom right corner) shows the shape of the $\wedge$-shaped source that replaces the black dot in the second example.

In our proposed approach, the reflection data contributes to the reconstruction of the multiple-scattering part of the virtual-source response.

Our objective is to retrieve the response originating from a virtual source inside an unknown medium, removing the imprint of a complex subsurface, as in seismic interferometry (Wapenaar et al., 2005; Curtis et al., 2006; Schuster, 2009). This is valuable in situations where waves have traveled inside a strongly inhomogeneous overburden, like a salt body (e.g., in subsalt imaging, Sava and Biondi, 2004). In this paper, we demonstrate that the requirement of having an actual receiver inside the medium can be circumvented, going beyond seismic interferometry.

We present numerical examples in a lossless acoustic medium with a syncline reflector, where the direct arrivals contain triplications. We discuss the influence of errors in the estimate of the first arrivals on the reconstructed wavefield. Such errors arise when a macro model (a routine product of velocity analysis) is used to compute the first arriving waveforms when such data are not available with other approaches, e.g., check shots or microseismic events. We then examine how the finite acquisition aperture and the limitations of the modeling code affect the results. While seismic interferometry usually deals with virtual point sources, this method allows us to reconstruct the response to a spatially-extended virtual source. This feature has a potential application in beam migration (Gray et al., 2009). Finally, we show that the proposed scheme implicitly reconstructs the incident field that fo-

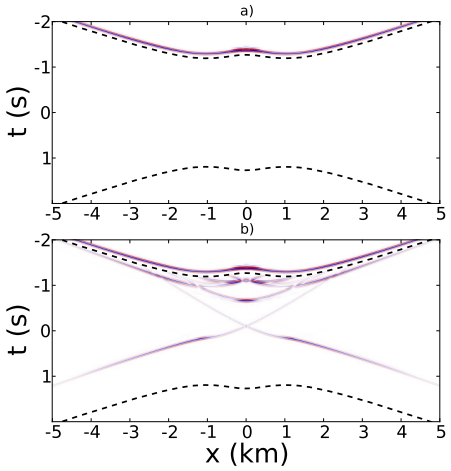

Figure 2: (a) Initial incident wavefield $p_0^+(\mathbf{x},t)$. (b) First iteration of the incident wavefield $p_1^+(\mathbf{x},t)$; this incident field will focus the wavefield at the virtual source location $\mathbf{x}_{VS}$ (black dot) in Figure 1a at $t=0$. We show the wavefield for $-2<t<2$ s only.

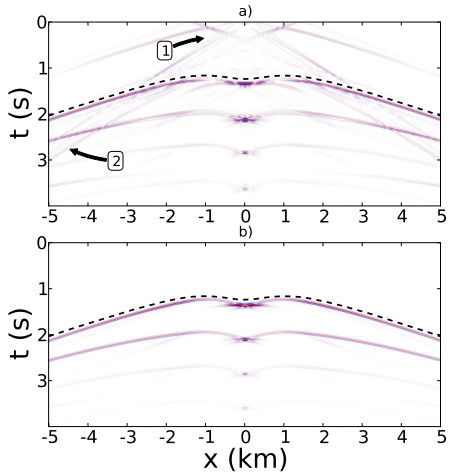

Figure 3: (a) Causal part of the superposition of the total field and its time-reversed version, $p_1(\mathbf{x},t)+p_1(\mathbf{x},-t)$. Label (1) indicates an incomplete cancellation of the events inside the window $w(\mathbf{x},t)$. Label (2) shows the effect of edge diffraction due to finite aperture. (b) Directly-modeled full response to the virtual source (black dot) shown in Figure 1a.

cuses the wavefield in time and space at the virtual source location.

ITERATIVE PROCESS AND NUMERICAL EXAMPLES

We require that the wavefield focuses at a specific location, hence the proposed method is not totally independent of knowledge about the medium. The iterative scheme requires the reflection response of the medium measured at the surface, complemented with independent information about the primary arrivals originated from the focusing location, to focus the acoustic wavefield inside the medium. The primary arrival wavefront can be estimated or measured in various ways: by forward modeling using a macro model, directly from the data by the Common Focusing Point method (CFP) (Thorbecke, 1997) when the virtual source is located at an interface, from microseismic events (Artman et al., 2010), or from borehole check shots. We denote the 2D spatial coordinates as $\mathbf{x}=(x,z)$. We assume that the reflection response does not include any multiples due to the free surface. Hence, $R(\mathbf{x}_R,\mathbf{x}_S,t)*s(t)$ can be obtained from reflection data measured at the recording surface $z=0$ after a surface-related multiple elimination processing (Verschuur et al., 1992), where $s(t)$ is a zero-phase wavelet.

We examine a configuration with a syncline reflector, whose velocity is shown in Figure 1a. The density profile (not shown) has a similar behavior and the densities of the three layers are $\rho_1=6500$ kg/m^3, $\rho_2=1000$ kg/m^3, and $\rho_3=7000$ kg/m^3, from top to bottom layer. The direct arriving wavefront associated with this model contains a triplication. To start the iterative scheme, we compute the direct arrivals originating from the virtual source using the macro model of Figure 1b. This is a smooth version of the velocity model of Figure 1a. We define the initial incident downgoing wavefield $p_0^+(\mathbf{x},t)$ at $z=0$ as the time-reversed version of the direct arrivals at the recording surface excited by the virtual source $\mathbf{x}_{VS}$. The initial incident wavefield is shown in Figure 2a. The subscript 0 in $p_0^+(\mathbf{x},t)$ denotes the 0th iteration (initial) of the incident wavefield. Note that, due to the smoothing, the triplications are not present in this field (i.e., the time-reversed version of the direct arrivals). In Figure 2a, we also define two traveltime curves, indicated by the dashed black lines. The upper curve follows directly after the initial incident wavefield $p_0^+(\mathbf{x},t)$ and the lower curve is the time-reversed version of the upper curve. These curves define a key component of the iterative scheme: the window function defined as

$$\begin{aligned} w(\mathbf{x},t)&=1 \quad \text{between the dashed black lines of Figure 2a}\\ w(\mathbf{x},t)&=0 \quad \text{elsewhere.} \end{aligned} \tag{1}$$

The upgoing reflection response $p_0^-(\mathbf{x},t)$ is obtained either by injecting the downgoing incident wavefield $p_0^+(\mathbf{x},t)$ into the actual medium or by convolving the downgoing incident wavefield $p_0^+(\mathbf{x},t)$ with the deconvolved reflection response and integrating over the source positions:

$$p_k^-(\mathbf{x}_R,t)=\int_{-\infty}^{\infty}\left[R(\mathbf{x}_R,\mathbf{x},t)*p_k^+(\mathbf{x},t)\right]_{z=0}dx, \tag{2}$$

for $\mathbf{x}$ and $\mathbf{x}_R$ at $z=0$, and $k=0$. Equation (2) is a Rayleigh-type integral (Wapenaar and Berkhout, 1993, equation 15a).

We discuss an iterative scheme that uses the (k-1)th iteration of the reflected wavefield $p_{k-1}^-(\mathbf{x},t)$ to construct the kth iteration of the downgoing incident field $p_k^+(\mathbf{x},t)$. The aim is to iteratively update the incident field $p_k^+(\mathbf{x},t)$ in such a way that, within the upper and lower dashed black lines shown in Figure 2a (i.e., inside the time window), the field is anti-symmetric in time. The meaning of this criterion will be clear in the remainder of this work, where we show the reconstruction of the response to a virtual source inside $\mathbf{x}_{VS}$. The proposed method uses a combination of time reversal and time windowing to construct the next iteration of the incident field. The kth iteration of the incident field $p_k^+(\mathbf{x},t)$ is specified by

$$p_k^+(\mathbf{x},t)=p_0^+(\mathbf{x},t)-w(\mathbf{x},t)p_{k-1}^-(\mathbf{x},-t), \quad \text{for } \mathbf{x} \text{ at } z=0, \tag{3}$$

where the time window $w(\mathbf{x},t)$ is defined by equation (1). We compute the initial response $p_0^-(\mathbf{x},t)$ injecting $p_0^+(\mathbf{x},t)$ into the actual medium, apply the window function $w(\mathbf{x},t)$, and construct

the first iteration of the updated incident wavefield $p_1^+(\mathbf{x},t)$ (see Figure 2b).

We define the superposition of the kth version of the incident and reflected wavefields as $p_k(\mathbf{x},t) = p_k^+(\mathbf{x},t) + p_k^-(\mathbf{x},t)$. Also, we define $p(\mathbf{x},t)$ as the final result of the iterative process. Note that, within the dashed black lines, the total field at $z = 0$ is antisymmetric in time and this particular feature was the design criterion for the iterative scheme. Hence, if we stack the total field and its time-reversed version, i.e., $p(\mathbf{x},t) + p(\mathbf{x},-t)$, all events inside the time window cancel each other. The causal part of $p(\mathbf{x},t)$ is equal to $p^-(\mathbf{x},t) + p^+(\mathbf{x},-t)$ and the anti-causal part corresponds to $p^+(\mathbf{x},t) + p^-(\mathbf{x},-t)$. From a physical point of view, time-reversal switches the direction of propagation, hence it follows that the causal part is upward propagating at $z = 0$ and the anti-causal part is downward propagating at $z = 0$.

For this particular configuration, we achieve the final result after only one iteration ($k = 1$). We form the field $p(\mathbf{x},t) + p(\mathbf{x},-t) = p_1(\mathbf{x},t) + p_1(\mathbf{x},-t)$ to reconstruct the response originating from the virtual source location. The causal part of this field is shown in Figure 3a. Labels (1) and (2) indicate an incomplete cancellation of events. This is possibly due to numerical limitations of the modeling code (e.g., numerical dispersion and influence of spatial-tapering on the incident field). The amplitude of the data shown in Figure 3 are clipped to 70% of the maximum amplitude and this enhances the features indicated by labels (1) and (2). The first event below the dashed curve of Figure 3a has the same arrival time of the direct arrival of the response to the virtual source at $\mathbf{x}_{VS}$. If we combine this last reasoning with the fact that the causal part propagates upward at $z = 0$, and that the total field is symmetric and obeys the wave equation in the inhomogeneous medium, it is reasonable that the total field in Figure 3a is proportional to the response due to a real source placed at the virtual source location $\mathbf{x}_{VS}$, as shown in Figure 3b. Work on a derivation of this principle is in progress.

The comparison between the two panels of Figure 3 shows that it is possible to reconstruct the full response to a virtual source inside the medium, including all multiples, using the direct arrivals computed using a smooth model. Note that this procedure is expected to converge because in each iteration the reflected energy is smaller than the incident energy. We interpret the proposed iterative method as a correction scheme that minimizes the energy of the wavefield inside the time window $w(\mathbf{x},t)$. Moreover, the proposed method does not take into account any particular feature of the model used in this analysis, hence it should hold for more general situations.

We simulate the propagation of the updated incident field $p_1^+(\mathbf{x},t)$ inside the medium of Figure 1a. Figure 4 displays six snapshots extracted from this simulation. Panel d shows that the wavefield collapsed to a focus at the location indicated by the black dot in Figure 1a. We note that the approximate direct arrivals (computed with the smooth model) used to start the iterative process caused an imperfect virtual source as indicated by the artifacts around the virtual source. Note that the complex wavefield propagating inside the syncline (panels a,b,c,e, and f) annihilates at the focusing time as shown in panel d.

Finally, we repeat similar steps for the same velocity model but

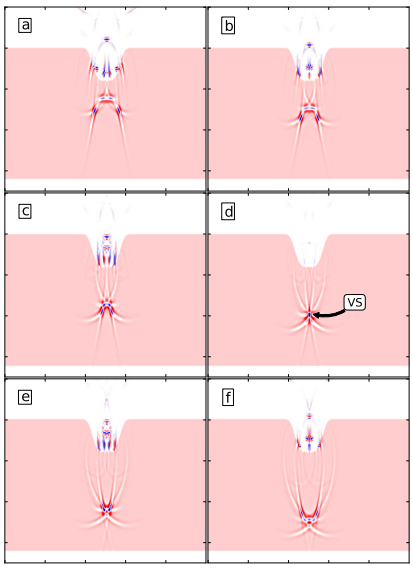

Figure 4: Time snapshots extracted from the propagating wavefield when the field of Figure 2b is used as a source. Panel d shows the wavefield focused at the location indicated by the black dot in Figure 1a. Time is increasing from panel a to f.

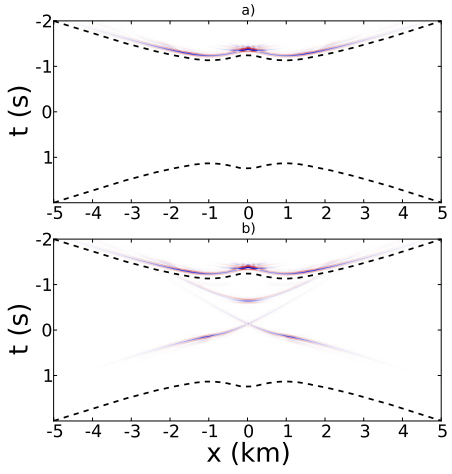

Figure 5: (a) Initial incident wavefield $p_0^+(\mathbf{x},t)$. (b) First iteration of the incident wavefield $p_1^+(\mathbf{x},t)$; this incident field will focus the wavefield at the virtual source location in Figure 1a at $t = 0$, when the $\wedge$-shaped virtual source replaces the black dot. We show the wavefield for the time interval $-2 < t < 2$ s.

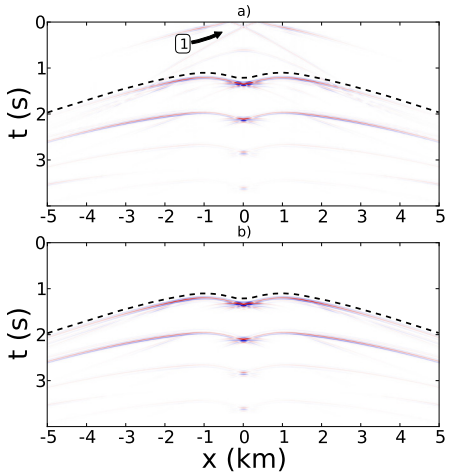

Figure 6: (a) Causal part of the superposition of the total field and its time-reversed version, $p_1(\mathbf{x},t)+p_1(\mathbf{x},-t)$. Label (1) indicates an incomplete cancellation of the events inside the window $w(\mathbf{x},t)$. (b) Directly-modeled full response to the $\wedge$-shaped virtual source shown in Figure 1a.

now use a spatially-extended virtual source, i.e., a $\wedge$-shaped source as shown in the square inset of Figure 1a. The $\wedge$-shaped source replaces the black dot used previously. In contrast to the first example, we compute the first arrivals using the true model instead of the smooth macro model. We do this to show that the quality and degree of focusing at the virtual source location depends on the first arrivals. Since the direct arrivals are now exact, Figure 7d shows that the wavefield focuses well on the target source. The proposed scheme produces a better result with less artifacts in this situation (compared to Figure 4d), because we have a correct estimate of the first arriving wavefront. Furthermore, the reconstructed response shown below the dashed curve in Figure 6a is virtually identical to the directly-modeled response shown in Figure 6b.

CONCLUSIONS

We discussed a generalization to two dimensions of the model-independent wavefield focusing and reconstruction method of Broggini et al. (2011, 2012) and Broggini and Snieder (2012). Unlike the 1D method, which uses the reflection response only, the proposed multi-dimensional extension requires, in addition to the reflection response, independent information about the first arrivals.

The proposed data-driven procedure yields the response to a virtual source (Figures 3a, 6a), removes the imprint of the subsurface (as the virtual source method), and reconstructs internal multiples, without needing a receiver at the virtual source location and without needing detailed knowledge of the medium. The method requires (1) the direct arriving wave front at the surface originated from a virtual source in the subsurface, and (2) the reflection impulse responses for all source and receiver positions at the surface. The direct arriving wave front can be obtained by modeling in a macro model, directly from the data by the CFP method (Berkhout, 1997) when the virtual source is located at an interface, from microseismic events (Artman et al., 2010), or from borehole

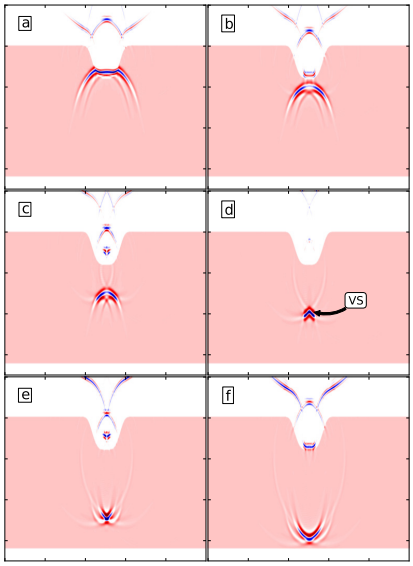

Figure 7: Time snapshots extracted from the propagating wavefield when the field of Figure 5b is used as a source. Panel d shows the wavefield focused at the location indicated by the $\wedge$-shaped symbol in Figure 1a. Time increases from panel a to f.

check shots. In the first numerical example, we used a smooth version of the true model to compute the direct arrivals. The required reflection impulse responses are obtained from seismic reflection data after surface-related multiple elimination (Verschuur et al., 1992) and deconvolution for the source wavelet.

We showed that the method is not limited to point sources, but also handles spatially-extended virtual sources. This feature permits to create and steer oriented beams originating at depth under a complex overburden that generates strong multiples. This beamforming process could have a potential use in beam migration (Gray et al., 2009). Errors in the estimated first arrivals (due to a smooth macro model) cause defocusing and a mislocalization of the virtual source (similar as in standard imaging algorithms). Such errors, however, do not affect the handling of the internal multiples and do not deteriorate their reconstruction, which is handled by the actual medium through the reflection data measured at the surface (that includes all the information about the medium itself). Note that also the virtual source method (Bakulin and Calvert, 2006) does not optimally focus the wavefield at the virtual source location, but Wapenaar et al. (2011b) show that the focusing can be improved applying multi-dimensional deconvolution. Furthermore, because the proposed method is non-recursive, the reconstruction of internal multiples will not suffer from error propagation, unlike other internal multiple suppression techniques used in seismic imaging.

ACKNOWLEDGMENTS

This work was supported by the sponsors of the Consortium Project on Seismic Inverse Methods for Complex Structures at the Center for Wave Phenomena and the Netherlands Research Centre for Integrated Solid Earth Science (ISES).

REFERENCES

Artman, B., I. Podladtchikov, and B. Witten, 2010, Source location using time-reverse imaging: Geophysical Prospecting, **58**, 861–873.

Bakulin, A., and R. Calvert, 2006, The virtual source method: Theory and case study: Geophysics, **71**, SI139–SI150.

Berkhout, A. J., 1997, Pushing the limits of seismic imaging, Part I: Prestack migration in terms of double dynamic focusing: Geophysics, **62**, 937–954.

Broggini, F., and R. Snieder, 2012, Connection of scattering principles: a visual and mathematical tour: European Journal of Physics, **33**, 593–613.

Broggini, F., R. Snieder, and K. Wapenaar, 2011, Connection of scattering principles: Focusing the wavefield without source or receiver: SEG Technical Program Expanded Abstracts, **30**, 3845–3850.

———, 2012, Focusing the wavefield inside an unknown 1D medium - Beyond seismic interferometry: submitted to Geophysics.

Curtis, A., P. Gerstoft, H. Sato, R. Snieder, and K. Wapenaar, 2006, Seismic interferometry—turning noise into signal: The Leading Edge, **25**, 1082–1092.

Gray, S. H., Y. Xie, C. Notfors, T. Zhu, D. Wang, and C.-O. Ting, 2009, Taking apart beam migration: The Leading Edge, **28**, 1098–1108.

Sava, P., and B. Biondi, 2004, Wave-equation migration velocity analysis - II: Subsalt imaging example: Geophysical Prospecting, **52**, 607–623.

Schuster, G. T., 2009, Seismic Interferometry: Cambridge University Press.

Thorbecke, J., 1997, Common Focus Point Technology: PhD thesis, Technische Universiteit Delft.

Verschuur, D. J., A. J. Berkhout, and C. P. A. Wapenaar, 1992, Adaptive surface-related multiple elimination: Geophysics, **57**, 1166–1177.

Wapenaar, K., and A. J. Berkhout, 1993, Representations of seismic reflection data. Part I: state of affairs: Journal of Seismic Exploration, **2**, 123–131.

Wapenaar, K., F. Broggini, and R. Snieder, 2011a, A proposal for model-independent 3D wave field reconstruction from reflection data: SEG Technical Program Expanded Abstracts, **30**, 3788–3792.

Wapenaar, K., J. Fokkema, and R. Snieder, 2005, Retrieving the Green's function in an open system by cross correlation: A comparison of approaches (L): Journal of the Acoustical Society of America, **118**, 2783–2786.

Wapenaar, K., E. Ruigrok, J. van der Neut, and D. Draganov, 2011b, Improved surface-wave retrieval from ambient seismic noise by multi-dimensional deconvolution: Geophys. Res. Lett., **38**, L01313.